

# Epitaxial thin films and heterostructures of a copper-oxide-based isotropic metallic oxide ( $\text{La}_{8-x}\text{Sr}_x\text{Cu}_8\text{O}_{20}$ )

C. B. Eom<sup>a)</sup>

Department of Mechanical Engineering and Materials Science, Duke University, Durham, North Carolina 27708

R. J. Cava, Julia M. Phillips, and D. J. Werder  
AT&T Bell Laboratories, Murray Hill, New Jersey 07974

(Received 5 April 1994; accepted for publication 11 January 1995)

Epitaxial thin films of a copper-oxide-based isotropic metallic oxide ( $\text{La}_{8-x}\text{Sr}_x\text{Cu}_8\text{O}_{20}$ ) and superconducting heterostructures ( $\text{YBa}_2\text{Cu}_3\text{O}_7/\text{La}_{8-x}\text{Sr}_x\text{Cu}_8\text{O}_{20}/\text{YBa}_2\text{Cu}_3\text{O}_7$ ) have been fabricated by  $90^\circ$  off-axis sputtering.  $\text{La}_{8-x}\text{Sr}_x\text{Cu}_8\text{O}_{20}$  is an oxygen-deficient pseudocubic perovskite that exhibits Pauli paramagnetism. X-ray diffraction and cross-sectional transmission electron microscopy reveal the heterostructures to have high crystalline quality and clean interfaces. This material will facilitate fabrication of ideal superconductor-normal-metal-superconductor Josephson junctions with low boundary resistance due to its excellent chemical compatibility and lattice match with cuprate superconductors and will be useful for determining the source of interface resistance in such heterostructures. © 1995 American Institute of Physics.

A critical technology issue in integrated high- $T_c$  superconducting devices is the choice of an appropriate metal for normal-metal barriers in superconductor-normal-metal-superconductor (SNS) Josephson junctions. A good metal for SNS junction barriers has low interface resistance to the superconductor, leads to good coupling with the superconductor, and has high bulk resistivity to maximize the  $I_c R_n$  product (critical current times junction resistance).<sup>1</sup> Epitaxial metallic oxide layers promise to yield the best device performance due to their excellent chemical and structural compatibility with cuprate superconductors. Furthermore, it is desirable to use "isotropic" materials for fabricating devices because one can then make the devices in any direction.

We have reported the first growth and characterization of single-domain epitaxial thin films of the isotropic metallic oxides  $\text{Sr}_{1-x}\text{Ca}_x\text{RuO}_3$  ( $0 \leq x \leq 1$ ).<sup>2</sup> Other researchers have also investigated different isotropic metallic oxide layers such as  $\text{La}_{0.5}\text{Sr}_{0.5}\text{CoO}_3$ ,<sup>3</sup>  $\text{LaNiO}_3$ ,<sup>4</sup>  $\text{LaCuO}_3$ ,<sup>5</sup> and  $\text{La}_4\text{BaCu}_5\text{O}_{20}$ .<sup>6</sup> These are pseudocubic perovskites with essentially isotropic properties. The resistivity of the thin films ranges from 100 to 400  $\mu\Omega$  cm at room temperature. Some of these metallic oxides have been used in SNS junctions. Char *et al.* fabricated SNS Josephson junctions with the trilayer edge geometry using  $\text{CaRuO}_3$  as the normal-metal barrier.<sup>7</sup> They found that unusually high interface resistance between the barrier and the superconductor raised the junction resistance by a factor of 10–100 above the bulk resistance of the barrier material, leading to nonuniform junction properties.

Recently, we have found various defects at the interfaces between YBCO and  $\text{Sr}_{1-x}\text{Ca}_x\text{RuO}_3$  through cross-sectional transmission electron microscopy (TEM) study of YBCO/ $\text{Sr}_{1-x}\text{Ca}_x\text{RuO}_3$  heterostructures.<sup>8</sup> Olsson and Char<sup>9</sup> also found small insulating  $\text{Y}_2\text{O}_3$  particles at the interfaces between  $\text{CaRuO}_3$  and YBCO in edge junctions. These interfacial defects may arise from chemical incompatibility of the

noncopper-oxide-based metallic oxide normal-metal barriers and the cuprate superconductors, and cause high interface resistances. In contrast, these kinds of interfacial defects have not been observed in superconducting heterostructures with other anisotropic copper-oxide-based materials such as in *c*-axis and *a*-axis YBCO/ $\text{PrBa}_2\text{Cu}_3\text{O}_7$  superlattices.<sup>10</sup> As an alternative, "copper-oxide-based isotropic" metallic oxides might be the ideal material for fabricating high-quality SNS junctions with low interface resistance.

In this communication we present results on epitaxial thin film layers of a new family of copper-oxide-based isotropic metallic oxides ( $\text{La}_{8-x}\text{Sr}_x\text{Cu}_8\text{O}_{20}$ ,  $x=1.6$ )<sup>11</sup> for the normal-metal barriers in SNS junctions. The material is an oxygen-deficient pseudocubic perovskite which differs from the stoichiometric perovskite  $\text{ABO}_3$  in its superstructure and in the number of oxygen vacancies.<sup>12</sup> Figures 1(a) and 1(b) show the projection onto the (001) plane of the framework of these oxygen deficient perovskites and a stoichiometric cubic perovskite ( $\text{ABO}_3$ ), respectively. Oxygen vacancies are ordered in  $\text{La}_{8-x}\text{Sr}_x\text{Cu}_8\text{O}_{20}$ , forming rows parallel to  $\langle 001 \rangle$ . The  $[\text{Cu}_8\text{O}_{20}]$  framework is built of corner-sharing  $\text{CuO}_6$  octahedra,  $\text{CuO}_5$  pyramids, and  $\text{CuO}_4$  square planar groups forming hexagonal tunnels in which the  $\text{La}^{3+}$  and  $\text{Sr}^{2+}$  ions are located. The mixed-valence character of copper is responsible for the metallic transport properties of this oxide.<sup>11</sup> The molar magnetic susceptibility is very weak and nearly independent of temperature. This suggests Pauli paramagnetism, which is ideal for a normal-metal barrier in SNS junctions because the material will not exhibit magnetic pair breaking.

The crystal symmetry of these materials is tetragonal, as outlined in Fig. 1(a). The lattice parameters of the tetragonal cell ( $a_0^T=10.79$  Å and  $c_0^T=3.862$  Å) are related to the lattice parameters of the perovskite cubic cell ( $a_0^P$  and  $c_0^P$ ) in the following way:  $a_0^T=2\sqrt{2}a_0^P$ ,  $c_0^T=c_0^P$ . The lattice parameters and distortion of the perovskite unit cell ( $a_0^P=3.81$  Å, and  $c_0^P=3.86$  Å) are very similar to those of YBCO ( $a_0=3.82$  Å,

<sup>a)</sup>Electronic mail: eom@acpub.duke.edu

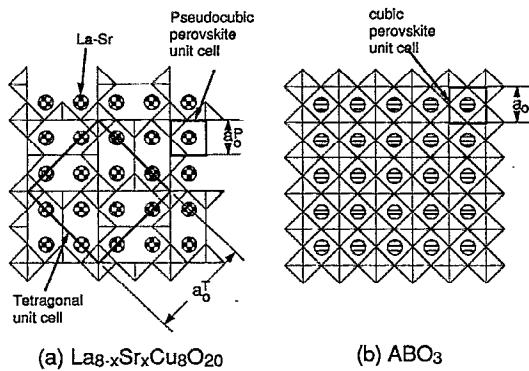


FIG. 1. Projection onto the (001) plane of the framework of (a) the oxygen-deficient perovskite ( $\text{La}_{6.4}\text{Sr}_{1.6}\text{Cu}_8\text{O}_{20}$ ) and (b) a stoichiometric cubic perovskite ( $\text{ABO}_3$ ) showing oxygen vacancy ordering. Copper coordination polyhedra as shown, tetragonal and perovskite unit cells outlined.

$b_0 = c_0/3 = 3.89 \text{ \AA}$ ), which will allow us to grow lower-stress heterostructures.

This family of copper-oxide-based isotropic metallic oxides has been previously studied only in bulk form. In order to use these materials for superconducting devices, we need them in epitaxial thin-film form. There are a number of issues that must be addressed before these materials can be used as a normal-metal barrier. First, the correct phase ( $\text{ABO}_{3-x}$  pseudocubic "113" phase) of the material must form on top of various layers (such as a substrate or YBCO) under *in situ* thin-film growth conditions (low oxygen partial pressure and low substrate temperature). It is already known that the  $\text{K}_2\text{NiF}_4$  layered phase ("214" phase) is much more stable than the  $\text{ABO}_3$  pseudocubic phase (113 phase) in the La-Sr-Cu-O system. Second, in order to fabricate multilayered device structures the growth of epitaxial heterostructures is required. Finally, the electrical and magnetic properties of the epitaxial thin films must be the same as in their bulk form.

We have grown single-layer thin films of  $\text{La}_{6.4}\text{Sr}_{1.6}\text{Cu}_8\text{O}_{20}$  on (100)  $\text{SrTiO}_3$  substrates *in situ* by a  $90^\circ$  off-axis sputtering technique, which produces films whose composition is nearly identical to that of the target.<sup>13,14</sup> The optimum growth temperature for  $\text{La}_{8-x}\text{Sr}_x\text{Cu}_8\text{O}_{20}$  thin films is substantially lower ( $610^\circ\text{C}$ ) than that used for *c*-axis YBCO thin films, which is desirable to minimize interdiffusion.

The film textures were investigated by x-ray diffraction with a four-circle diffractometer. Figure 2(a) shows the  $\theta$ - $2\theta$  scan of a  $\text{La}_{6.4}\text{Sr}_{1.6}\text{Cu}_8\text{O}_{20}$  thin film grown on a (100)  $\text{SrTiO}_3$  substrate. The only substantial peaks detected are from *d* spacings corresponding to  $\{h00\}^{P\ddagger\ddagger}$  of the  $\text{La}_{6.4}\text{Sr}_{1.6}\text{Cu}_8\text{O}_{20}$  (113) pseudocubic phase. ( $P\ddagger\ddagger$  defines Miller indices based on a pseudocubic perovskite subcell. This is the same as  $\{hh0\}^T$  based on a tetragonal unit cell. Peaks are indexed based on both unit cells.) Because of a large tetragonal splitting in this structure, it is possible to determine from the normal  $\theta$ - $2\theta$  scan alone whether the texture is (100), (001), or a combination. The inset clearly shows the absence of (002)-oriented grains of  $\text{La}_{6.4}\text{Sr}_{1.6}\text{Cu}_8\text{O}_{20}$ . We therefore conclude that these films have a purely (100)<sup>P</sup> texture normal to the substrate. The  $(n + 1/2, 0, 0)^P$  peaks (where  $n = 0, 1, \text{ and } 2$ )

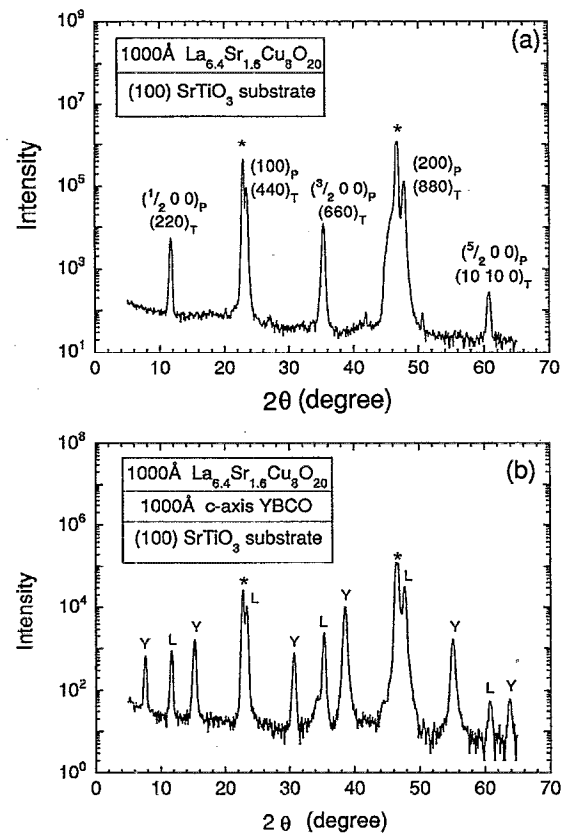


FIG. 2. (a) X-ray-diffraction  $\theta$ - $2\theta$  scan on a  $\text{La}_{6.4}\text{Sr}_{1.6}\text{Cu}_8\text{O}_{20}$  thin film on (100)  $\text{SrTiO}_3$ . (b) X-ray-diffraction  $\theta$ - $2\theta$  scan on a  $\text{La}_{6.4}\text{Sr}_{1.6}\text{Cu}_8\text{O}_{20}$ /YBCO heterostructure on (100)  $\text{SrTiO}_3$ . The  $\text{SrTiO}_3$  substrate, YBCO, and  $\text{La}_{6.4}\text{Sr}_{1.6}\text{Cu}_8\text{O}_{20}$  peaks are marked as \*, Y, and L, respectively.

are not allowed in stoichiometric cubic perovskites but arise from the superstructure due to oxygen vacancy ordering in the (001) plane. The measured lattice parameter of the perovskite unit cell normal to the substrate is  $3.81 \text{ \AA}$ , which is the same as the bulk value. The  $\omega$  scan rocking curve width (FWHM) of the  $\{220\}$  reflections of  $\text{La}_{6.4}\text{Sr}_{1.6}\text{Cu}_8\text{O}_{20}$  is  $0.16^\circ$  and is limited by instrumental resolution. The films grown at high temperature (above  $700^\circ\text{C}$ ) show predominantly the  $\text{La}_{2-x}\text{Sr}_x\text{Cu}_4$  (214) phase with an (001) texture.

We have measured normal state resistivities of the thin films as a function of temperature by the four-terminal transport method. Figure 3 shows a resistivity versus temperature curve for a  $1000\text{-\AA}$ -thick  $\text{La}_{6.4}\text{Sr}_{1.6}\text{Cu}_8\text{O}_{20}$  film on (100)  $\text{SrTiO}_3$ . The resistivity behavior along the two orthogonal directions is the same, which is expected since this is an isotropic material. The resistivity at room temperature ( $\rho_{300}$ ) is  $\sim 700 \mu\Omega \text{ cm}$ , and the temperature dependence ( $d\rho/dT$ ) shows good metallic behavior which is similar to those of three-dimensional metals.

We have made and characterized two types of bilayers on (100)  $\text{SrTiO}_3$ . First, we made  $1000 \text{ \AA}$   $\text{La}_{6.4}\text{Sr}_{1.6}\text{Cu}_8\text{O}_{20}$  on top of  $1000 \text{ \AA}$  YBCO. X-ray diffraction exhibited only  $(h00)^P$  peaks of  $\text{La}_{6.4}\text{Sr}_{1.6}\text{Cu}_8\text{O}_{20}$  and  $(00l)$  peaks of YBCO, showing good epitaxy of the normal-metal barrier layer [see Fig. 2(b)]. Next, we made  $1000 \text{ \AA}$  YBCO on top of  $1000 \text{ \AA}$   $\text{La}_{6.4}\text{Sr}_{1.6}\text{Cu}_8\text{O}_{20}$ . X-ray diffraction also exhibited only  $(h00)^P$  peaks of  $\text{La}_{6.4}\text{Sr}_{1.6}\text{Cu}_8\text{O}_{20}$  and  $(00l)$  peaks of YBCO,

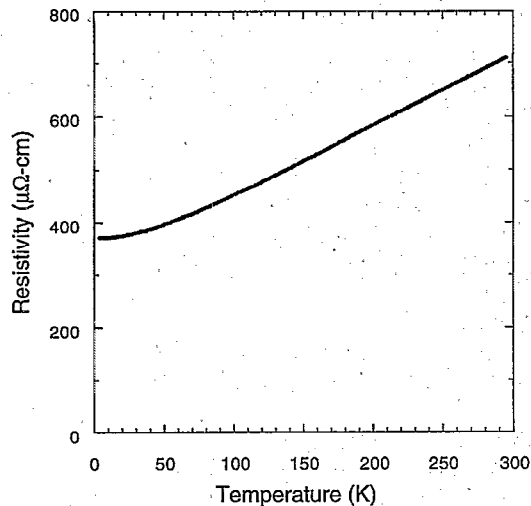


FIG. 3. Resistivity vs temperature curve for a 1000-Å-thick  $\text{La}_{6.4}\text{Sr}_{1.6}\text{Cu}_8\text{O}_{20}$  thin film on (100)  $\text{SrTiO}_3$ .

showing good epitaxy. Superconducting transition temperatures of YBCO layers in these bilayer structures are as good as those of single-layer YBCO thin films on (100)  $\text{SrTiO}_3$  substrates.

We have prepared a trilayer heterostructure with a normal-metal barrier thickness of 350 Å. Figure 4 is a low-magnification cross-sectional TEM image of *c*-axis YBCO/ $\text{La}_{6.4}\text{Sr}_{1.6}\text{Cu}_8\text{O}_{20}$ /*c*-axis YBCO on (100)  $\text{SrTiO}_3$ . It shows two types of  $\text{La}_{6.4}\text{Sr}_{1.6}\text{Cu}_8\text{O}_{20}$  domains with in-plane epitaxial arrangements of  $\text{La}_{6.4}\text{Sr}_{1.6}\text{Cu}_8\text{O}_{20}$  (001)<sup>P</sup>//YBCO (100)// $\text{SrTiO}_3$  (100) and  $\text{La}_{6.4}\text{Sr}_{1.6}\text{Cu}_8\text{O}_{20}$  (010)<sup>P</sup>//YBCO (100)// $\text{SrTiO}_3$  (100), which was also confirmed by off-axis x-ray  $\Phi$  scans of (201)<sup>P</sup> reflections. The thickness of the  $\text{La}_{6.4}\text{Sr}_{1.6}\text{Cu}_8\text{O}_{20}$  layer is very uniform with less than 20 Å variation. A high-magnification TEM image (see an inset) shows very clean interfaces between YBCO and  $\text{La}_{6.4}\text{Sr}_{1.6}\text{Cu}_8\text{O}_{20}$ . This is in contrast to the defective interfaces observed in heterostructures of several noncopper-oxide-based isotropic metallic oxide layers such as  $\text{CaRuO}_3$  and  $\text{SrRuO}_3$ .<sup>8</sup>

The superconducting coherence length in high- $T_c$  superconductors is extremely small ( $\sim 10$  Å in the *a*-*b* plane). Therefore, even a small amount of disorder at the interface between a superconductor and a normal-metal barrier will be detrimental to junction properties. In order to obtain reproducible and uniform junction properties, control of the interface on an atomic scale is required. During the growth of YBCO/ $\text{La}_{8-x}\text{Sr}_x\text{Cu}_8\text{O}_{20}$ /YBCO trilayer structures the structural and chemical coherency at the interface will be maintained because the basic building block of both materials is Cu-O. In contrast, noncopper-oxide-based isotropic metallic oxides such as  $\text{CaRuO}_3$  do not have any chemical coherency at the interface. For example, interdiffusion of Ca or Ru ions into the YBCO layer can occur, which is very harmful to interface-sensitive junction properties. Therefore,  $\text{La}_{8-x}\text{Sr}_x\text{Cu}_8\text{O}_{20}$  and other copper-oxide-based isotropic metallic oxides might be the preferred normal metals for SNS junctions.

In summary, we have grown single-phase epitaxial thin

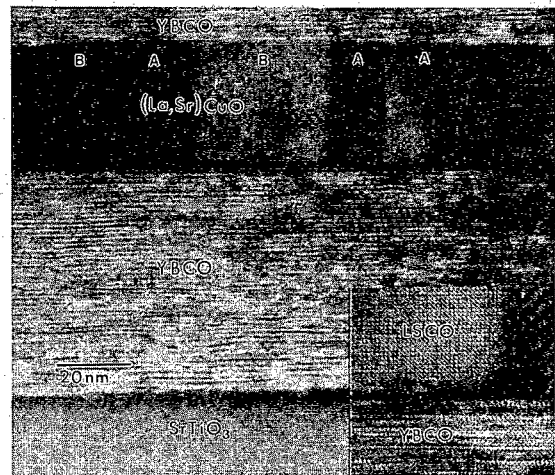


FIG. 4. Cross-sectional TEM micrograph of a *c*-axis YBCO/ $\text{La}_{6.4}\text{Sr}_{1.6}\text{Cu}_8\text{O}_{20}$ /*c*-axis YBCO SNS heterostructure. Domains with (001) and (010) normal to image are indicated as A and B, respectively. The inset shows a high-magnification image near the YBCO and  $\text{La}_{6.4}\text{Sr}_{1.6}\text{Cu}_8\text{O}_{20}$  interface.

films of a new (in thin-film form) copper-oxide-based isotropic metallic oxide ( $\text{La}_{8-x}\text{Sr}_x\text{Cu}_8\text{O}_{20}$ ) and heterostructures with YBCO. This material should facilitate fabrication of ideal SNS Josephson junctions with low interface resistance and uniform junction properties due to its excellent chemical and structural compatibility with cuprate superconductors. It will also help elucidate the origin of interface resistance; we therefore may be able to control important junction properties such as  $I_c$  and  $R_n A$ .

We would like to thank C. H. Chen for helpful discussions. We also thank J. H. Marshall, J. J. Krajewski, W. F. Peck, Jr., and R. A. Rao for technical assistance and target preparation.

- <sup>1</sup> M. Y. Kupriyanov and K. K. Likharev, *IEEE Trans. Magn.* **MAG-27**, 2460 (1991).
- <sup>2</sup> C. B. Eom, R. J. Cava, R. M. Fleming, J. M. Phillips, R. B. van Dover, J. H. Marshall, J. W. P. Hsu, J. J. Krajewski, and W. F. Peck, Jr., *Science* **258**, 1766 (1993).
- <sup>3</sup> J. T. Cheung, P. E. D. Morgan, D. H. Lowndes, X.-Y. Zheng, and J. Breen, *Appl. Phys. Lett.* **62**, 2045 (1993).
- <sup>4</sup> K. M. Satyalakshmi, R. M. Mallya, K. V. Ramanathan, X. D. Wu, B. Brainard, D. C. Gautier, N. Y. Vasanthacharya, and M. S. Hedge, *Appl. Phys. Lett.* **62**, 1233 (1993).
- <sup>5</sup> K. Char, M. S. Colcough, T. H. Geballe, and K. E. Myers, *Appl. Phys. Lett.* **62**, 196 (1993).
- <sup>6</sup> A. Gupta, B. W. Hussey, A. M. Guloy, T. M. Shaw, R. F. Saraf, J. F. Bringley, and B. A. Scott, *J. Solid State Chem.* **108**, 202 (1994).
- <sup>7</sup> R. Desfeux, J. F. Hamot, B. Mercey, C. Simon, M. Hervieu, and B. Raveau, *Physica C* **221**, 205 (1994).
- <sup>8</sup> C. B. Eom, R. M. Fleming, J. M. Phillips, R. J. Cava, J. H. Marshall, D. J. Werder, C. H. Chen, J. J. Krajewski, and W. F. Peck, Jr., *MRS Spring Meeting Abstract*, 1993, p. 401.
- <sup>9</sup> E. Olsson and K. Char, *Appl. Phys. Lett.* **64**, 1292 (1994).
- <sup>10</sup> C. B. Eom, A. F. Marshall, J.-M. Triscone, B. Wilkens, S. S. Laderman, and T. H. Geballe, *Science* **251**, 780 (1991).
- <sup>11</sup> L. Er-Rakho, C. Michel, and B. Raveau, *J. Solid State Chem.* **73**, 514 (1988).
- <sup>12</sup> J. F. Bringley, B. A. Scott, S. J. La Placa, R. F. Boehme, T. M. Shaw, M. W. McElfresh, S. S. Trail, and D. E. Cox, *Nature* **347**, 263 (1990).
- <sup>13</sup> C. B. Eom, J. Z. Sun, K. Yamamoto, A. F. Marshall, K. E. Luther, T. H. Geballe, and S. S. Laderman, *Appl. Phys. Lett.* **55**, 595 (1989).
- <sup>14</sup> C. B. Eom, J. Z. Sun, B. M. Lairson, S. K. Streiffer, A. F. Marshall, K. Yamamoto, S. M. Anlage, J. C. Bravman, S. S. Laderman, R. C. Taber, R. D. Jacowitz, and T. H. Geballe, *Physica C* **171**, 351 (1990).